Neoplasia • Vol. 6, No. 2, March/April 2004, pp. 106–116 106

www.neoplasia.com

Interleukin-12 Inhibits Tumor Growth in a Novel Angiogenesis Canine Hemangiosarcoma Xenograft Model[1]

Nasim Akhtar[*,2], *Marcia L. Padilla*[*,2], *Erin B. Dickerson*[*], *Howard Steinberg*[†], *Matthew Breen*[‡], *Robert Auerbach,*[§,¶] *and Stuart C. Helfand*[*,¶]

Departments of *Medical Sciences and [†]Pathobiological Sciences, School of Veterinary Medicine, University of Wisconsin-Madison, Madison, WI, USA; [‡]Department of Molecular Biomedical Sciences, College of Veterinary Medicine, North Carolina State University, Raleigh, NC, USA; [§]Laboratory of Developmental Biology, University of Wisconsin-Madison, Madison, WI, USA; [¶]University of Wisconsin Comprehensive Cancer Center, Madison, WI, USA

Abstract

We established a canine hemangiosarcoma cell line derived from malignant endothelial cells comprising a spontaneous tumor in a dog to provide a renewable source of endothelial cells for studies of angiogenesis in malignancy. Pieces of the hemangiosarcoma biopsy were engrafted subcutaneously in a bg/nu/XID mouse allowing the tumor cells to expand *in vivo*. A cell line, SB-HSA, was derived from the xenograft. SB-HSA cells expressed vascular endothelial growth factor (VEGF) receptors 1 and 2, CD31, CD146, and $\alpha_v\beta_3$ integrin, and produced several growth factors and cytokines, including VEGF, basic fibroblast growth factor, and interleukin (IL)-8 that are stimulatory to endothelial cell growth. These results indicated that the cells recapitulated features of mitotically activated endothelia. *In vivo*, SB-HSA cells stimulated robust angiogenic responses in mice and formed tumor masses composed of aberrant vascular channels in immunocompromised mice providing novel opportunities for investigating the effectiveness of antiangiogenic agents. Using this model, we determined that IL-12, a cytokine with both immunostimulatory and antiangiogenic effects, suppressed angiogenesis induced by, and tumor growth of, SB-HSA cells. The endothelial cell model we have described offers unique opportunities to pursue further investigations with IL-12, as well as other antiangiogenic approaches in cancer therapy.

Neoplasia (2004) **6**, 106–116

Keywords: Angiogenesis, endothelial cell, malignant, dog, cytokine.

Introduction

Angiogenesis, the formation of new blood vessels from preexisting vessels, has been intensively studied over the past several decades because of its fundamental importance in tissue development, vascular diseases, and cancer. Angiogenesis is most active during fetal development, whereas after birth, it is an important physiological function in the ovary and placenta, and in wound healing. Pathological angiogenesis that is inappropriate and unregulated is a prominent feature of malignancy that facilitates tumor growth and metastasis. Improved treatment of malignancies that have progressed to the proangiogenic phenotype requires relevant models to test the safety and efficacy of innovative antiangiogenic therapies. Systems to study angiogenesis in the laboratory are limited by the transient nature of angiogenic events and limited accessibility to angiogenic tissues. Sources of endothelial cells currently used in the laboratory include human umbilical vein, and bovine aorta, pulmonary vein, and pulmonary artery [1–3]. A malignant hemangioendothelioma of murine origin is also used for studying endothelial cell biology [4]. Other endothelial cells, such as those derived from bovine adrenal cortex and retina, rat brain, mouse aorta, epididymal fat pad, thoracic duct, or liver, have been more difficult to maintain in stable long-term culture [5–7]. In addition, several human endothelial cell lines have been immortalized by transfection or retroviral transduction with the human telomerase reverse transcriptase gene (reviewed in Bouis et al. [8]).

In order to understand the developmental processes and functions of normal cells, neoplastic cells have been used because tumor cells are capable of proliferating both *in vitro* and *in vivo* and, at the same time, can maintain many of the properties of their normal counterparts. For example, plasmacytomas have provided material that has led to the characterization of Ig structure, and studies of teratomas have helped to clarify how differentiation takes place [4]. In the same way, endothelial cells derived from tumors or endothelial cell tumors can be used to understand the biology of endothelial cells. There is a potential advantage to a renewable source of

Address all correspondence to: Stuart C. Helfand, School of Veterinary Medicine, University of Wisconsin, 2015 Linden Drive, Madison, WI 53706-1102, USA.
E-mail: helfands@svm.vetmed.wisc.edu

[1]Supported by National Institutes of Health grants CA86264, CA14520, and P30 CA14520-29, and AKC/CHF grant 2025 (S.C.H.).
[2]Equal contribution.
Received 15 September 2003; Revised 1 December 2003; Accepted 3 December 2003.

DOI 10.1593/neo.03334

endothelial cells for study because primary endothelial cells have a limited lifespan and display characteristics that differ from batch to batch due to their multidonor origin [8]. We established a canine hemangiosarcoma cell line derived from malignant endothelial cells comprising a spontaneous subcutaneous tumor in a dog. These cells possess characteristics typical of the endothelium, including surface expression of vascular endothelial growth factor (VEGF) receptors 1 and 2, CD31, CD146, $\alpha_v\beta_3$ integrin, and others, and produce several factors including VEGF, basic fibroblast growth factor (bFGF), and interleukin (IL)-8 that are stimulatory to endothelial cell growth. *In vivo*, the cells stimulate robust angiogenic responses in mice and form tumor masses composed of aberrant vascular channels in immunocompromised mice, providing excellent opportunities for investigating the effectiveness of antiangiogenic agents.

Using this model, we determined that IL-12, a cytokine with both immunostimulatory and antiangiogenic effects, suppressed both tumor-associated angiogenesis and growth of canine hemangiosarcoma *in vivo*. Tumor growth delay of the malignant endothelial cells may have been due to suppression of tumor-induced neovascularization by IL-12, direct suppression of malignant endothelial hemangiosarcoma cell growth by IL-12, activation of tumoricidal NK cells, or a combination of mechanisms. Taken together, these studies report a valuable new model for investigating angiogenesis and demonstrate a promising role for IL-12 in controlling the growth of angiogenic tumors.

Materials and Methods

Source of Malignant Endothelial Cells

A 9-year–old German shepherd dog presented to the Veterinary Medical Teaching Hospital (VMTH) at the University of Wisconsin School of Veterinary Medicine (UW-SVM) was euthanized for an enlarging 20-cm fluctuant subcutaneous mass over the left shoulder. The mass had previously been biopsied and diagnosed as a hemangiosarcoma, a malignancy of endothelial cells, by a board-certified veterinary pathologist. Immediately following euthanasia, a small piece of tumor was excised and used as the source of tissue to develop the current studies. All procedures were performed in accordance with a protocol approved by the Animal Care and Use Committee of the UW-SVM.

Mice

BALB/c and NOD-SCID mice were purchased from Jackson Laboratories (Bar Harbor, ME) and bg/nu/XID mice were purchased from Harlan (Indianapolis, IN). BALB/c and NOD-SCID mice were subsequently bred in a colony at the UW-SVM. The bg/nu/XID mice were used in experiments following receipt from the vendor. All mice were 8 to 12 weeks old when used in experiments.

Development of SB-HSA Malignant Endothelial Cell Line

Several small pieces (< 0.5 cm diameter) of the hemangiosarcoma biopsy were engrafted subcutaneously in the dorsal cervical area of a bg/nu/XID mouse. The mouse was anesthesized with intraperitoneal injection of avertin (tribromoethanol/tertiary amyl alcohol [1:1] diluted to 2% in 10% ethyl alcohol, 0.1 ml/10 g of body weight). The fur was clipped and the skin cleansed with 70% ethanol. A small skin incision was made and a subcutaneous pocket was created by blunt dissection. Tumor pieces washed in phosphate-buffered saline (PBS) were introduced into the pocket and the skin wound closed. Following recovery, the mouse was monitored for 120 days, at which time a 1-cm-diameter tumor was present and the animal was sacrificed. The tumor was excised and a portion was snap-frozen with liquid nitrogen in Tissue Tek OCT compound (Sakura Finetek USA, Torrance, CA) for immunohistochemical staining and the remainder was used for establishing a primary canine hemangiosarcoma cell line. The tumor tissue was minced and transferred to a flask containing a modified enzyme dissociation solution and glass beads, as described [9]. The enzyme dissociation solution consisted of 270 U/ml type I collagenase (Invitrogen Life Technologies, Baltimore, MD), 200 U/ml DNAse from bovine pancreas (Sigma, Indianapolis, IN), and penicillin–streptomycin (10,000 IU/ml penicillin and 10 mg/ml streptomycin) solution 1% vol/vol (Mediatech, Inc., Cellgro, Herndon, VA) dissolved in Minimal Essential Medium Eagle with Earle's balanced salt solution (BioWhittaker, Walkersville, MD). Tissue pieces were incubated at 37°C in a 5% humidified CO_2 atmosphere with gentle agitation using a magnetic stirrer. After approximately 1 hour, the suspension was allowed to stand for a few minutes in order for the larger undissociated pieces to settle. The top suspension was collected and passed through a 40-μm nylon mesh cell strainer and centrifuged at 400*g* for 8 to 10 minutes. The cell pellet was washed with PBS depleted of Mg and Ca (dPBS) and centrifuged at 400*g* for 8 to 10 minutes. Red blood cells were lysed with an ammonium chloride lysing buffer and the wash step was repeated. The cell pellet was resuspended in RPMI 1640 medium supplemented with 10% heat-inactivated fetal bovine serum, 1% vol/vol penicillin–streptomycin solution, 2 mM sodium pyruvate, 2 mM L-glutamine, and 10 mM HEPES buffer (Sigma-Aldrich, St. Louis, MO); transferred to a 75-cm^2 tissue culture flask; and incubated overnight at 37°C in a humidified 5% CO_2 atmosphere. At that time, the medium was aspirated and the adherent cells were gently washed with PBS before endothelial growth medium (EGM-2; BioWhittaker) was added to the flask. The cells were expanded in EGM-2 medium and passaged when confluent.

After 14 passages, the cells were sorted by direct two-color immunofluorescence labeling (described in Flow Cytometry section). The brightest 10% of the cells labeling positive for expression of $\alpha_v\beta_3$ integrin and CD146 were collected, cultured in EGM-2 medium, and expanded. When sufficient cell numbers were available, 5×10^6 cells were injected subcutaneously into the dorsum of a bg/nu/XID mouse and allowed to grow until a 1-cm^3 tumor developed after 30 days. The mouse was euthanized and the tumor was excised. Once again, a portion was snap-frozen in OCT compound for immunohistochemical staining and the

remaining tumor was used to establish a single-cell suspension using the method described above, then sorted a second time for bright staining of $\alpha_v\beta_3$ integrin and CD146. The brightest cells were collected and plated in 75-cm^2 flasks in EGM-2 medium for expansion. These cells, called the SB-HSA cell line developed from the second passage in a bg/nu/XID mouse, were used for all experiments (Figure 1). Aliquots of early passages were frozen in liquid nitrogen.

Flow Cytometry

Cell sorting and flow cytometric analysis of the SB-HSA cell line were done by direct two-color immunofluorescence labeling using a FACSCalibur cell sorter or a FACScan flow cytometer (Becton Dickinson, San Jose, CA). For cell sorting and flow cytometry, fluorescein isothiocyanate (FITC)– or phycoerythrin (PE)–conjugated monoclonal antibodies (mAbs) specific for two endothelial cell surface antigens were used. Murine mAb P1H12 (IgG1; Chemicon International, Temecula, CA) that recognizes CD146, an endothelial surface antigen [10], was conjugated to FITC, and mAb LM609 (murine IgG1; Chemicon), which recognizes $\alpha_v\beta_3$ integrin (CD51/CD61) in numerous species [11–18], including the dog but not the mouse (Chemicon LM609 Datasheet and confirmed in our laboratory), was conjugated to PE.

Briefly, SB-HSA cells were washed with HBSS and detached with 5 mM EDTA. Cells were then collected with EGM-2 medium and centrifuged at 400*g* for 5 minutes. The cell pellet was washed with dPBS and centrifuged at 400*g* for 5 minutes. The washed cells were resuspended in 1 ml of dPBS and counted using a hemocytometer. Cells were further diluted with cold dPBS containing 1% bovine serum albumin (BSA) and adjusted to a concentration of 5×10^6/ml, and 50 μl (2.5×10^5 cells) was placed into microcentrifuge tubes for staining. mAbs (5 μg/ml) were added to individual tubes and the cells were incubated at 4°C in the dark for 30 minutes, then washed with cold dPBS containing 1% BSA. FITC- or PE-conjugated irrelevant mouse IgG1 antibodies (3 μl/2×10^5 cells) were used as isotype controls. Propidium iodide was added just before cell analysis as a live–dead discriminator. Ten thousand events were collected and analyzed with the CellQuest v.3.3 software package (Becton Dickinson). Additional antibodies used in flow cytometry experiments included rat antimouse c-kit (CD117; Pharmingen, San Diego, CA) conjugated to PE and an irrelevant rat antimouse IgG2b conjugated to PE as its control.

SB-HSA Tumor Xenograft

Canine hemangiosarcoma xenografts were established in NOD-SCID mice by injection of 5×10^6 SB-HSA cells

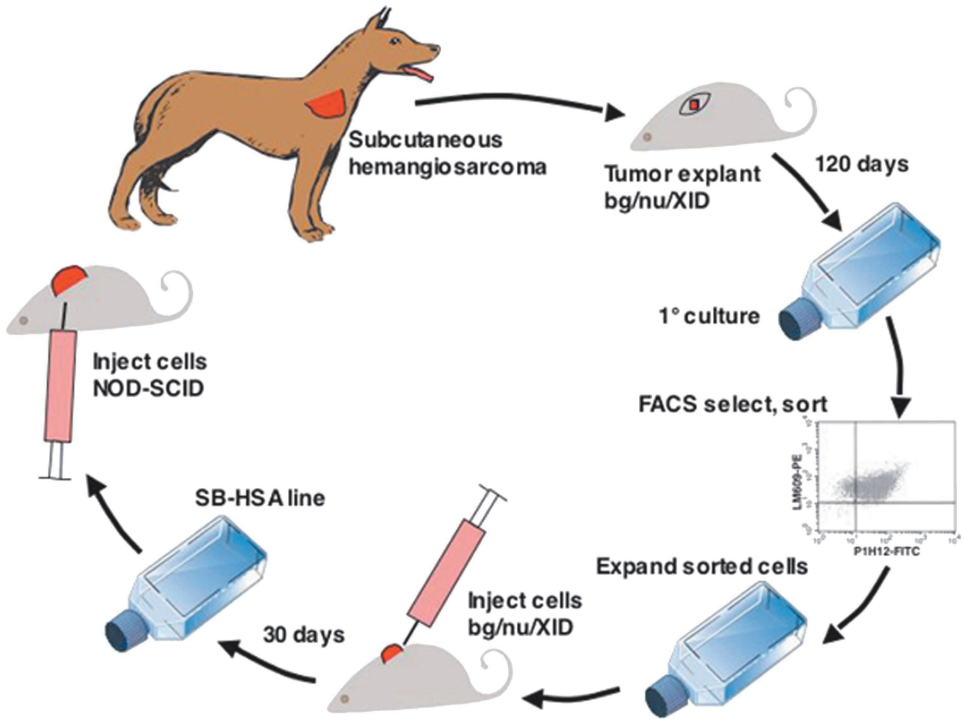

Figure 1. *Establishment of a canine hemangiosarcoma (HSA) xenograft model. A biopsy was taken from a subcutaneous HSA of the right shoulder of a 9-year–old German shepherd dog. Several small pieces of the HSA biopsy were engrafted subcutaneously in the dorsal cervical area of a bg/nu/XID mouse and the skin wound was sutured closed. The mouse was monitored for 120 days, at which time a 1-cm-diameter tumor was present and the animal was sacrificed. The tumor was excised and a portion was snap-frozen with liquid nitrogen in OCT compound for immunohistochemical staining and the remainder was used for establishing the primary canine HSA cell line. After 14 passages, the cells were sorted and cells labeling positive for expression of α_{v3} integrin (with a canine-selective antibody) and CD146 (P1H12) were collected and expanded. About 5×10^6 cells were injected subcutaneously into the dorsum of a second bg/nu/XID mouse and allowed to grow for 30 days until a 1-cm^3 tumor had developed. The tumor was then excised. A portion was snap-frozen in OCT compound for immunohistochemical staining, and the remaining tumor was used to establish a single-cell suspension that was then expanded. These cells, called the SB-HSA cell line developed from the second passage in a bg/nu/XID mouse, were used for the remainder of the experiments to induce tumors in NOD-SCID mice.*

suspended in 200 μl of PBS over the dorsum using a 26-gauge needle and tuberculin syringe. Mice were examined every other day until tumors were detected and could be measured with calipers. Animals were sacrificed when tumors reached a size of 1 cm^3. In some experiments, 5×10^6 SB-HSA cells were injected intravenously into the tail vein.

Pathology

Gross and histopathological examinations of tissues from experimental mice were performed by a board-certified veterinary pathologist (H.S.). For histological examination, routine hematoxylin and eosin staining of fixed sections was done.

Immunohistochemistry

Immunohistochemical staining was performed on fresh frozen and formalin-fixed paraffin-embedded sections from SB-HSA tumors obtained from bg/nu/XID and NOD-SCID mice. Antibody clone P1H12 (anti-CD146; Chemicon) and LM609 (anti–$\alpha_v\beta_3$ integrin [CD51/CD61]; Chemicon) were used on fresh frozen sections, whereas mouse anti–human PECAM-1 (anti-CD31, clone JC/70A; Dako, Carpinteria, CA) and rabbit anti–human factor VIII polyclonal antibody (von Willebrand's factor; Signet, Dedham, MA) were used on fixed tissue sections following antigen retrieval. The final product was developed using alkaline phosphatase with New Fuchsin as the chromogen (Histo-Mark Red kit; Kirkegaard and Perry Laboratories, Gaithersburg, MD), as described [19,20]. Immunohistochemistry was performed by IHC Services (Smithville, TX; J. Wojcieszyn, PhD).

Fluorescence In Situ Hybridization (FISH)

FISH—using a panel of canine bacterial artificial chromosome (BAC) clones representing single-locus probes for chromosomes X, Y, and 26, and a BAC clone representing the canine tumor-suppressor gene *PTEN*—was employed to confirm the genetic identity of SB-HSA cells. Probe labeling, FISH, and image acquisition were performed as previously described [21]. Briefly, chromosome preparations were generated from the cell line when the cells were ~70% confluent. A conventional approach of colcemid arrest followed by hypotonic (75 mM KCl) and fixation (3:1 methanol:glacial acetic acid) treatments was used.

Reverse Transcription Polymerase Chain Reaction (RT-PCR)

Total RNA was extracted from SB-HSA cells with TRIzol reagent (Invitrogen Life Technologies) and reverse transcription was performed using SuperScript First Strand Synthesis Systems for RT-PCR (Invitrogen Life Technologies) according to the manufacturer's instructions. The PCR products were separated using a 1% agarose gel, stained with ethidium bromide, and visualized with ultraviolet (UV) light. Conditions used to detect messages of interest in endothelial cells are shown in Table 1.

Corneal Angiogenesis Assay

Polyvinyl sponges (Rippey, Eldorado Hills, CA) preirradiated with 2000 Gy of gamma irradiation (cesium source) were cut into $4 \times 4 \times 2$ mm pieces, and 70,000 SB-HSA

Table 1. RT-PCR Conditions

cDNA	Primers* (Forward: 5′–3′; Reverse: 5′–3′)	Thermal Cycler Program†	PCR Product (bp)
VEGF	CCATGAACTTTCTGCTCTCTTGTTG TCTTGCTCTATCTTTCTT	95°C, 1 min; 60°C, 1 min; 72°C, 1 min	450
VEGFR-1 (flt)	AAGCAGCCCATTCATGGTCTTTGCCCA TCAGGGATCAGGGTATCAAG	95°C, 1 min; 58°C, 1 min; 72°C, 1 min	380
VEGFR-2 (flk)	ACTGGAGCCTACAAGTGCTTCTAC/TTC/TT TCTTGGTCATCAGC/TCCACTG	95°C, 1 min; 59°C, 30 sec; 72°C, 1 min	650
bFGF	CTTCAAGGACCCCAGCGGCGCTCTT AGCAGACTTGG	94°C, 30 sec; 55°C, 30 sec; 72°C, 1 min	400
IL-8	TCAGAACTTCGATGCCAGTTTCAC GGATCTTGTTTCTC	94°C, 1 min; 52°C, 1 min; 72°C, 1 min	227
MMP-2	CCGTATGAGATCAAGCAGATTTACGG GTCCTCAATATCGAG	94°C, 30 sec; 56°C, 30 sec; 72°C, 30 sec	450
MMP-13	ATCTGTATGAGGAAGACTGACCAGAAG GTCCATCAA	94°C, 30 sec; 53°C, 30 sec; 72°C, 30 sec	450
SCF	CCAGAGTCAGTGTCACAAAACCCTTCTT CCAGTATAAGGCTCC	94°C, 1 min; 58.5°C, 1 min; 72°C, 1 min	196
c-Kit	CACCCTGGTCATTACAGAATATTGCGG AAGCCTTCCTTGATCATCTTG	95°C, 30 sec; 58°C, 30 sec; 72°C, 30 sec	650
β-Actin	CATGTTTGAGACATTCAACACCCCGCC ATCTCTTGCTCGAAGTCCAG	95°C, 1 min; 50°C, 1 min; 72°C, 1 min	325

*All primers were canine-specific sequence except β-actin, which was a human-specific sequence.

†Thirty-five cycles were used for all amplifications except β-actin cDNA, which was amplified by 30 cycles. All conditions used a 95°C to 96°C 2-minute hot start with the exception of c-kit and β-actin. A final 7-minute extension at 72°C was used for all conditions, after which samples were held at 4°C. The concentration of $MgCl_2$ was 1.5 mM in all conditions except VEGF, IL-8, and c-kit, where it was 3 mM. VEGFR-1 was cloned in our laboratory (GenBank accession no. AF262963).

cells were introduced into the sponges. BALB/c mice were anesthesized with Avertin and a small surgical micropocket was created in the center of the avascular cornea. Sponges were then inserted into the micropocket. Eyes were examined for neovascularization daily using an ophthalmic microscope (Carl Zeiss, Inc., Thornwood, NY). On day 14 after implantation, 200 μl of FITC-conjugated high-molecular-weight dextran (2,500,000 M_w, 200:1; Sigma) (FITC–dextran) was injected into the tail vein, and the animal was sacrificed 5 minutes later. The eyeball was enucleated from the orbital cavity and fixed for 5 minutes in 4% paraformaldehyde. The cornea with the adjacent limbus was dissected, rinsed in PBS, and mounted on a glass slide in 10% glycerol. Phase contrast and fluorescence microscopy were used to visualize the general layout of the cornea and the presence of perfused blood vessels, respectively [22,23]. A computer program (Powerpoint; Microsoft, Redmond, WA) was used to quantitate the percentage of the image containing fluorochrome-labeled vessels through comparison of pixel counts above background.

Subcutaneous Matrigel/Sponge Assay

A sponge/Matrigel assay was used to visualize the angiogenic reaction induced by SB-HSA cells in the subcutaneous microenvironment, as described [24]. Matrigel (500 μl, 500:1; BD Biosciences, Bedford, MA) was injected subcutaneously with a 27-gauge needle in the flank region of 2.5- to 3.5-month–old BALB/c mice and allowed to solidify for 30 to 60 minutes. At that time, mice were anesthesized with Avertin given intraperitoneally. The fur overlying the Matrigel plug was clipped, the skin cleansed with betadine, and a stab incision was made over the Matrigel bleb. A stab incision was then made directly into the Matrigel plug and a sterilized polyvinyl sponge (3 × 2 × 1.5 mm) containing 1×10^5 SB-HSA tumor cells was introduced through the nick in the Matrigel and advanced to the center of the plug with a thumb forceps. The skin wound was closed with a 6-0 nylon suture and the mouse recovered under a heat lamp. Mice were observed after 24 hours to monitor the condition of the wound.

After 2 weeks, 200 μl of FITC–dextran was injected through the tail vein. Mice were euthanized 3 to 5 minutes later; the Matrigel plug was removed, separated from the abdominal skin and muscle, and fixed in 10% formalin. Phase contrast microscopy was used to examine the topography of the Matrigel plug, and the perfused blood vessels were visualized using fluorescence illumination.

Treatment of SB-HSA Tumor-Bearing Mice with IL-12

NOD-SCID mice were injected subcutaneously over the dorsum with SB-HSA cells (5×10^6 cells/200 μl). Two days later, they were anesthesized and osmotic pumps (Alzet Corporation, Palo Alto, CA) containing 33.3 μg in 200 μl of murine recombinant (mr) IL-12 (Peprotech, Rocky Hill, NJ) or 200 μl of PBS were inserted subcutaneously through a small flank skin incision. The skin wound was closed with wound clips. Pumps were designed to deliver 6 μl/day (1 μg/day IL-12) for 4 weeks. The mice were examined every other day for tumor development. Two perpendicular diameters were measured with calipers and tumor volume was calculated using the formula $(Dd^2)\pi / 6$, with D as the largest and d as the smallest diameters.

Statistical Analyses

Comparisons between tumor size and angiogenic responses of mice treated with IL-12 or PBS were made using a two-sample Wilcoxon test. A P value $\leq .05$ was considered significant.

Results

Flow Cytometry

Dissociated tumor cells obtained from the primary canine hemangiosarcoma tumor explant in a NOD-SCID mouse showed bright staining with mAb P1H12 (anti-CD146) and LM609 (anti–$\alpha_v\beta_3$ integrin) (Figure 1). P1H12 recognizes an antigen expressed chiefly by endothelial cells [10]. LM609 recognizes an adhesion molecule found on mitotically active endothelial cells. Although the species specificity of LM609 is broad, notably, it does not bind to $\alpha_v\beta_3$ integrin in the mouse. Taken together, the staining pattern exhibited by the cells derived from the primary tumor explant supports an endothelial nonmurine cell type consistent with the canine hemangiosarcoma transplanted to the first mouse. The brightest 10% of dually fluorescent cells (dot plot, upper right quadrant; Figure 1) were collected aseptically and expanded in culture to establish the SB-HSA cell line, as described in Materials and Methods section. This cell line was then used in the remainder of the experiments.

SB-HSA Tumor Xenograft

Cohorts ($n = 2, 4, 6, 12$) of NOD-SCID mice injected with SB-HSA cells typically developed large (1 cm^3) subcutaneous tumors 3 to 4 weeks after cells were injected (Figure 2). When tumors reached this size, mice were euthanized in accordance with animal use guidelines. Grossly, the tumors formed expansile infiltrative masses that were adherent to, and invading, the musculature deep to the subcutis. The overlying skin was also adhered to the tumor. The tumors were firm, lobulated, reddish/maroon masses that bled readily on cut surface (Figure 2). The gross appearance of lungs from these animals was considered to be normal. Mice ($n = 3$) that received only intravenous injections of SB-HSA cells through the tail vein were sacrificed after 2 months and found to have multifocal maroon tumor nodules (5 mm diameter) disseminated throughout the lungs (Figure 2) as well as an occasional larger (1 cm) subcutaneous tumor.

Histopathology

The tumor tissue was comprised of clusters of small sheets of pleiomorphic elongate plump spindle cells frequently forming slit-like spaces, many of which contained erythrocytes (Figure 3). The cells comprising these foci were polygonal to spindle-shaped, with small amounts of eosinophilic cytoplasm, usually indistinct cell margins, high

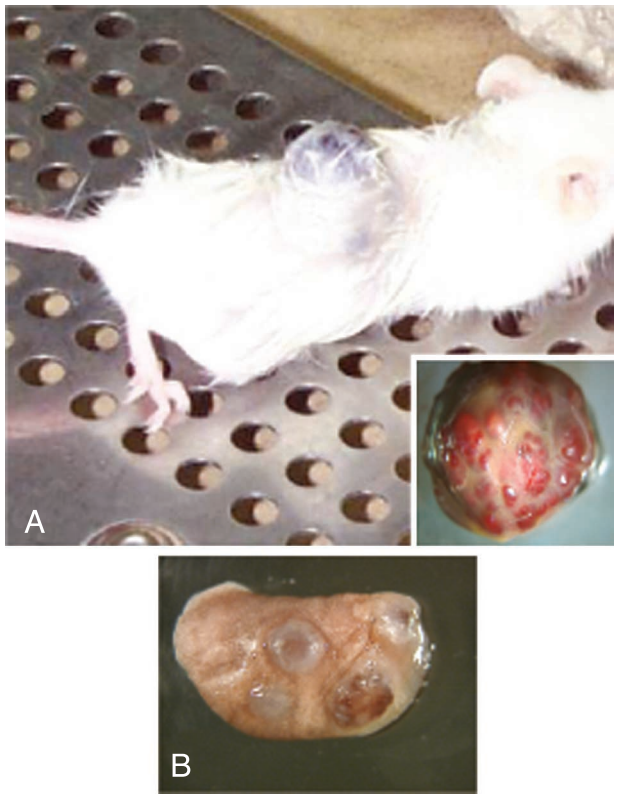

Figure 2. *SB-HSA cells produce tumors in immunodeficient mice. (A) Injection of 5 × 10^6 SB-HSA cells subcutaneously into NOD-SCID mice routinely produced large tumors within 3 to 4 weeks. Such a tumor has grown on the dorsal midline of the mouse in this photo. Inset: The gross appearance of SB-HSA tumors from NOD-SCID mice exhibits features indistinguishable from hemangiosarcoma in the dog. There is a characteristic bright red/maroon color to the tumor and the tumor bled excessively when cut. The tumor was highly vascular. Although implanted in the subcutaneous tissue, the tumors were invasive into the underlying musculature. (B) NOD-SCID mice were injected intravenously with 70,000 SB-HSA cells through the tail vein. After 2 months, mice were sacrificed and found to have multifocal maroon tumor nodules (5 mm diameter) disseminated throughout the lungs. This route of administration routinely produced pulmonary metastases.*

nuclear-to-cytoplasmic ratios, with oval variably sized nuclei with finely stippled chromatin, and variably sized multiple nucleoli. There were two mitotic figures per high-power field. The microscopic features were indistinguishable from canine hemangiosarcoma.

Immunohistochemistry

Immunohistochemical staining on fresh frozen and fixed tumor tissue from NOD-SCID mice showed positive staining of the tumor cells with antibodies P1H12 (anti-CD146), PECAM-1 (anti-CD31), and factor VIII, confirming the endothelial nature of the tumor (Figure 4). The cells also showed specific staining with LM609 (anti–$\alpha_v\beta_3$ integrin).

FISH

FISH analysis of SB-HSA chromosome preparations from cultured SB-HSA cells yielded hybridization signal for all of the canine-specific probes tested, indicating that the chromosomes were of canine origin (data not shown).

RT-PCR

RT-PCR was used to assess expression of message for several endothelial cell growth factors, receptor tyrosine kinases, and matrix metalloproteinases (MMPs) in SB-HSA cells (Figure 5*A*). Using primers designed from canine gene sequences, SB-HSA cells were found to express message for proangiogenic proteins including VEGF, bFGF, and IL-8. Message for receptor tyrosine kinases VEGFR-1 and VEGFR-2 and c-kit were also expressed as was the message for stem cell factor (SCF), the ligand for c-kit. Expression of c-kit has been associated with cells of the endothelial lineage. SB-HSA cells also expressed message

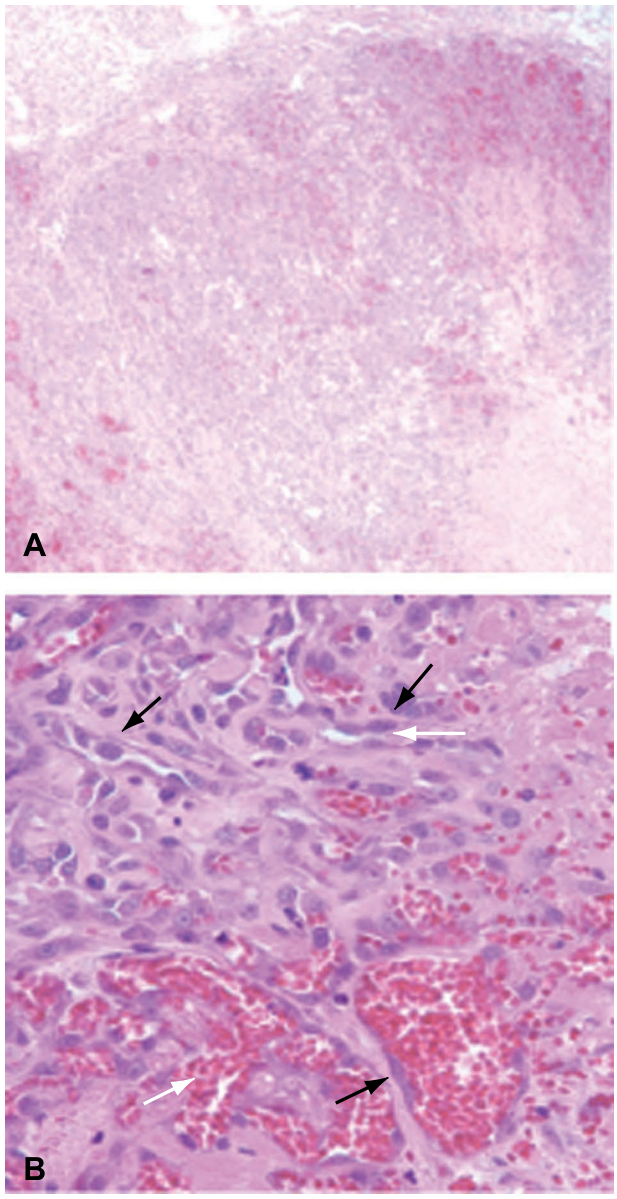

Figure 3. *SB-HSA tumors in NOD-SCID mice are histologically identical to canine hemangiosarcoma. The histological appearance of SB-HSA tumors grown in NOD-SCID mice, shown above, is indistinguishable from naturally occurring hemangiosarcoma in the dog. At low (× 40) power (A), there are sheets of tumor cells with blood-filled spaces and areas of necrosis (light pink, lower right). At high (× 400) power (B), plump atypical endothelial cells (black arrows) can be seen forming tortuous vascular spaces (white arrows).*

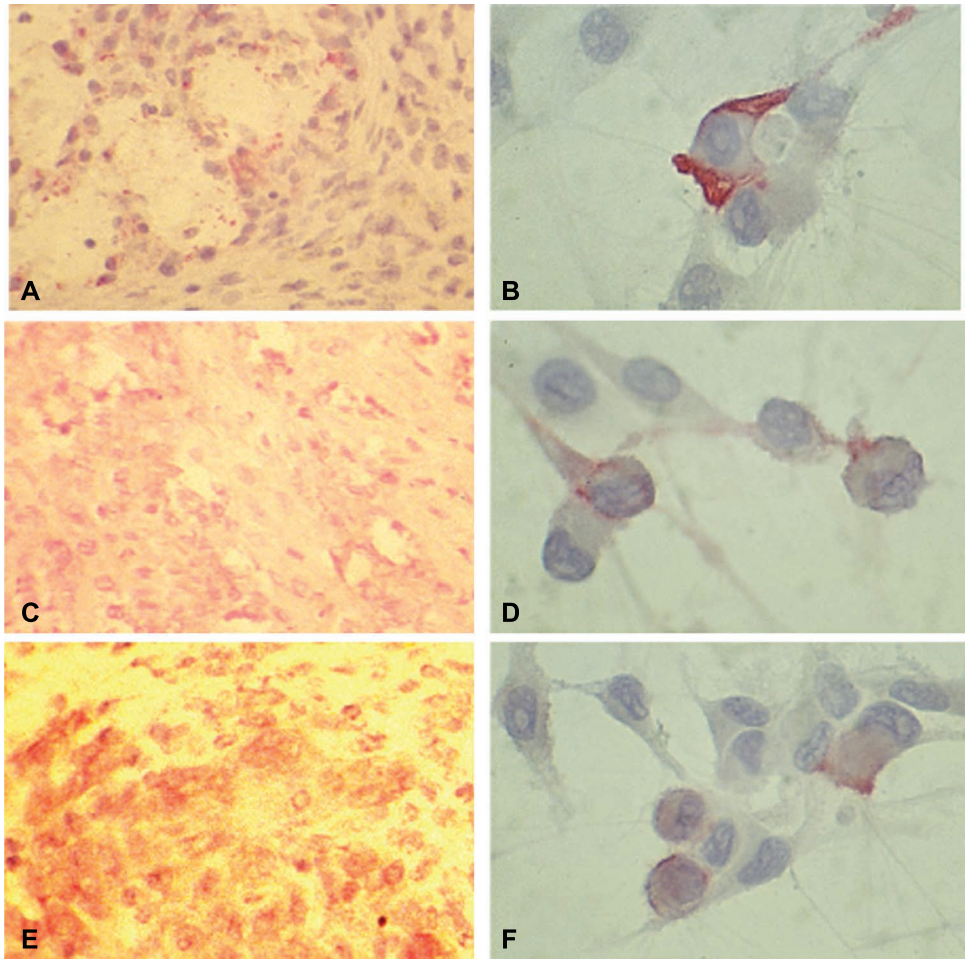

Figure 4. *Immunohistochemical staining confirms endothelial lineage of SB-HSA cells. Immunohistochemical staining was performed on fresh frozen and formalin-fixed, paraffin-embedded sections from SB-HSA tumors obtained from bg/nu/XID and NOD-SCID mice. Anti–factor VIII polyclonal antibody (A and B) and anti-CD31 (C and D) were used on fixed tissue sections following antigen retrieval, and P1H12 (E and F) was used on fresh frozen sections. The final product was developed using alkaline phosphatase with New Fuchsin as the chromogen. Positive staining is appreciated as a red color. Expression of these markers supports an endothelial lineage for the cells comprising the SB-HSA tumor. Original magnification, ×40 (panels A, C, and E) and × 100 (panels B, D, and F).*

for MMP-2 and MMP-13. These results suggest that SB-HSA hemangiosarcoma cells express proteins and receptors capable of stimulating endothelial cell growth and the ability for SB-HSA cells to promote their own growth in an autocrine and/or paracrine manner. In addition, MMP expression suggests that the cells are capable of altering the extracellular matrix, providing a mechanism for expansion and invasion. Flow cytometry using an anti–c-kit antibody was positive, demonstrating that protein was expressed for at least one of the transcripts amplified by RT-PCR from SB-HSA cells (Figure 5*B*).

Angiogenesis Assays

Two *in vivo* assays were used to assess the angiogenic properties of SB-HSA cells. The rationale for performing these experiments was based on the angiogenic profile revealed for this cell line by RT-PCR, which predicted the capacity of SB-HSA cells to stimulate new vessel growth. Further, hemangiosarcoma, being a malignancy of endothelial cells, is likely to be highly adapted to sustaining the needs for endothelial cell growth. In the corneal angiogenesis assay, sponges containing SB-HSA cells implanted onto the avascular cornea of BALB/c mice induced marked neovascularization, with neovessels advancing from the limbus toward the sponge (Figure 6*A*). Vessel ingrowth was detectable by 2 days following placement of the sponge, with vessels reaching the sponge by 12 days. Vessels were large and tortuous, with numerous points of arborization. Control corneas receiving sponge implants but without SB-HSA cells did not show neovascularization. In the subcutaneous sponge/Matrigel assay in BALB/c mice, vascular invasion of the Matrigel plug arising from the periphery and progressing centrally toward the sponge was detectable after 1 week. By 2 weeks, there was marked arborization of the infiltrating blood vessels that formed a network surrounding the sponge containing the SB-HSA cells (Figure 6*B*). Control sponge/Matrigel implants lacking these tumor cells failed to elicit a vascular response. These results confirmed that SB-HSA cells are strong inducers of angiogenesis.

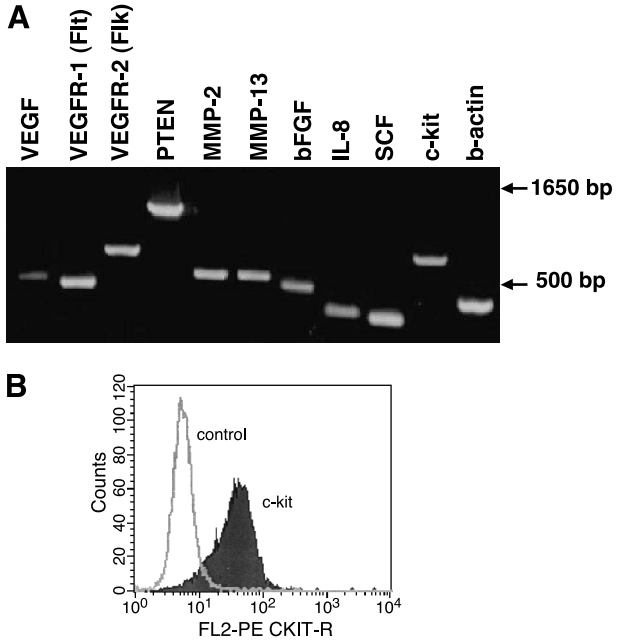

Figure 5. *Expression of endothelial growth factors and receptors by SB-HSA cells. (A) RT-PCR was used to detect messenger RNA for endothelial cell growth factors (VEGF, bFGF, and IL-8) and some of their receptors (VEGFR-1 and VEGFR-2). Other molecules of interest included PTEN, MMPs (MMP-2 and MMP-13), and c-kit. Primers were designed using canine sequences and β-actin was used as a control. Expression of VEGFR-1 and VEGFR-2 is considered selective for cells of the endothelial lineage. (B) Flow cytometry using an anti–c-kit antibody demonstrated bright expression of c-kit by SB-HSA cells confirming that the protein was expressed for one of the transcripts amplified by RT-PCR.*

IL-12 Suppresses Angiogenesis Induced by SB-HSA Cells In Vivo

The corneal pocket angiogenesis assay was also used to determine whether IL-12 could suppress angiogenesis induced by SB-HSA cells. Cohorts ($n = 5$) of BALB/c mice were randomized to receive either mrIL-12 (1 μg/day) or PBS. Each was delivered as a continuous subcutaneous infusion by osmotic pumps implanted subcutaneously 2 days after sponges containing 70,000 SB-HSA cells were placed into corneas as described above. After 1 week of treatment, mice were injected with FITC–dextran and euthanized, and the corneas were examined. Compared to the PBS-treated control group (Figure 6*C*), IL-12–treated mice showed significantly ($P < .05$) less corneal neovascularity (Figure 6*D*) as evidenced by markedly reduced corneal fluorescence. These results prove that IL-12 mediates a strong antiangiogenic effect against malignant endothelial cells that are capable of inducing robust neovascularization.

IL-12 Suppresses Growth of SB-HSA Tumors In Vivo

IL-12 is a cytokine with pleiotropic effects, including suppression of angiogenesis due to *in vivo* inhibition of endothelial cell growth. This activity is mediated by downstream chemokines such as IP-10 and Mig, which are induced by interferon-γ in response to IL-12. We evaluated the capacity of IL-12 to suppress the growth of SB-HSA tumors in NOD-SCID mice and, in so doing, explored the potential to use the inhibition of SB-HSA tumor development as a surrogate marker for suppression of endothelial cell growth and angiogenesis. Control mice that were injected subcutaneously with SB-HSA cells and received PBS developed tumors at the site of cell inoculation by the second week, which progressively enlarged over the 4-week observation period (Figure 7). In contrast, the growth of tumors in mice that received the continuous subcutaneous infusion of IL-12 was initially suppressed for 2 weeks followed by slower growth and significantly ($P = .016$) smaller size by the end of the 4-week observation period (Figure 7).

Discussion

We successfully established a transplantable endothelial tumor in mice derived from a spontaneous endothelial malignancy in a dog. When injected subcutaneously, cultured cells derived from the canine tumor repeatedly produced locally invasive endothelial cell tumors in mice. Intravenous injection of cells into the tail vein resulted in growth of disseminated tumor nodules throughout the lungs and other sites. The pattern of immunohistochemical antibody reactivity confirmed tumors to be endothelial and not derived from murine tissues, whereas FISH analyses further validated the cells to be of canine origin. Identification of growth factors and receptors potentially important for mediating autocrine and paracrine cell growth helped to shed light on putative growth pathways important for the survival of SB-HSA cells. Moreover, the array of receptors we investigated by RT-PCR is consistent with pathways known to be important to endothelial cell growth. Thus, the endothelial model we have described has the potential for studying angiogenesis as well as for investigating strategies to modulate angiogenesis in cancer. Although *in vivo* angiogenesis assays are time-consuming and more complicated than *in vitro* assays, they are essential because they preserve the complexities of angiogenesis that no *in vitro* system can duplicate [25]. Given the relative paucity of endothelial cell models available for studying angiogenesis, the system we have described has unique merits in this field. Inhibition of SB-HSA cell growth and metastasis by potential antiangiogenic agents can be useful to assess the activity of these compounds. It must be kept in mind, however, that the underlying cells in this model are malignant and may therefore differ from the normal endothelial cells from which they arose. In this respect, they exhibit characteristics that may be common to normal endothelial cells, while at the same time exhibiting features that deviate from the normal characteristics of the nontransformed endothelial parent cells.

This endothelial model was developed from a canine hemangiosarcoma. Hemangiosarcoma arises from transformed vascular endothelial (blood vessel) cells [26]. This tumor represents 7% of all canine malignancies, and it is more commonly seen in male dogs between 8 and 10 years old. German shepherd dogs are at greatest risk for hemangiosarcoma, but Golden Retrievers, Great Danes, boxers, English setters, and pointers are also overrepresented

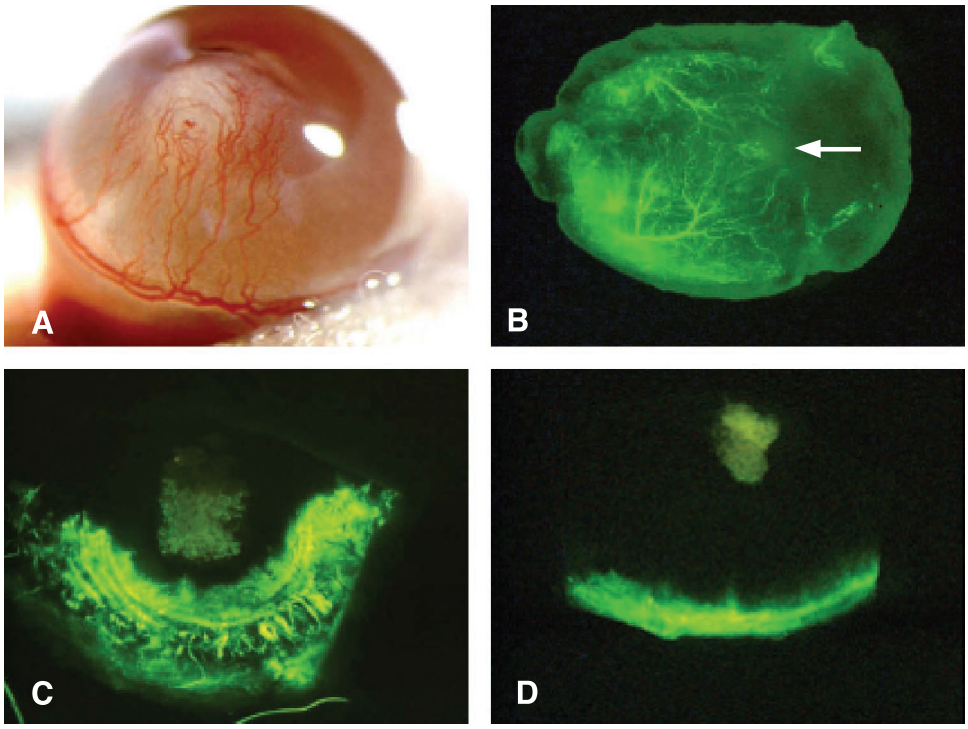

Figure 6. *SB-HSA cells are potent inducers of angiogenesis and IL-12 inhibits this effect. (A) A polyvinyl sponge containing 70,000 SB-HSA cells was placed into a surgically created corneal pocket in a BALB/c mouse. After 12 days, a robust angiogenic response is visible in the cornea, with neovascularization arising from the limbus and proceeding toward the sponge implant (white structure in the center of the cornea). Implanted sponges that did contain SB-HSA cells failed to provoke an angiogenic response. Experiment shown is representative of eight mice, all exhibiting a similar response. (B) Matrigel, an artificial connective tissue matrix, was injected subcutaneously in the flank of a BALB/c mouse. After solidifying, a nick was made into the Matrigel through a skin incision, and a polyvinyl sponge (arrow) containing 5 × 10^6 SB-HSA cells was inserted into the Matrigel. After 2 weeks and 3 to 5 minutes prior to sacrifice, 200 μl of FITC–dextran was injected into the tail vein and the Matrigel plug was removed. Under fluorescence microscopy, a pronounced angiogenic response was observed (arborized fluorescent green vessels), which progressed toward the proliferating SB-HSA cells in the sponge. These experiments confirm the proangiogenic properties of SB-HSA cells. The effect of IL-12 on SB-HSA–induced corneal angiogenesis was compared in BALB/c control mice given PBS (C) by continuous subcutaneous infusion versus BALB/c that received 1 μg/day mrIL-12 for 7 days by continuous subcutaneous infusion (D). Mice treated with IL-12 had significantly less corneal neovascularization compared to the control mice ($P < .05$). Mice were injected with FITC–dextran just prior to euthanasia and corneal vessels were evaluated with fluorescence microscopy. In this example, there was a 56% reduction in corneal neovascularization in the IL-12–treated mouse. The fluorescent vessel in the ventral aspect of the cornea in (D) is the normal limbic vessel and the green squares in the centers of (C) and (D) are the SB-HSA sponges that have absorbed fluorescein. Note that vessels have nearly reached the sponge in (C) whereas the cornea in (D) remains relatively avascular.*

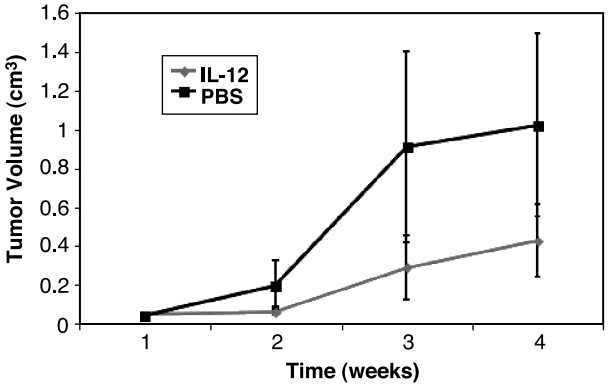

Figure 7. *IL-12 suppresses growth of canine hemangiosarcoma. Cohorts (n = 7) of NOD-SCID mice were injected subcutaneously with 5 × 10^6 SB-HSA cells over the dorsal thorax. Two days later, mice were anesthesized and small osmotic pumps containing PBS or murine recombinant IL-12 (IL-12) were inserted subcutaneously in the mice from respective cohorts. The pumps were designed to deliver continuous subcutaneous infusion of 6 μl/day for 4 weeks. The mice in the IL-12 group each received 1 μg/day IL-12 during that time period. At the conclusion of the study, the pumps were examined to verify that the contents had been delivered. Compared to the control (PBS) group, tumors in the mice that received IL-12 were significantly smaller ($P = .016$). Bars are standard errors.*

breeds [27,28]. The spleen, right atrium, and subcutis are the most common sites for primary hemangiosarcoma in dogs [26]. Local infiltration and systemic metastases are the common growth patterns [26,28]. Metastatic sites are widespread, with the lung and liver being the most frequently affected organs [26–28]. Splenic rupture results in tumor implants throughout the abdomen [28]. Morbidity and mortality are often due to acute internal hemorrhage secondary to rupture of highly vascular blood-filled tumors [28]. Despite surgery and intensive chemotherapy, the median survival time for dogs diagnosed with hemangiosarcoma is little more than 6 months [29,30].

Endothelial tumors have been described in humans, although less commonly than in the dog. In comparison to dogs, human angiosarcomas are rare and more commonly present as cutaneous tumors arising on the face and scalp [31,32]. Similar to the dog, however, their clinical course is aggressive and lethal due to metastases.

We identified a number of growth factor pathways in SB-HSA cells, some of which have generated keen interest as potential sites for antiangiogenic therapeutic intervention in

cancer. Therefore, the SB-HSA xenograft model may open additional avenues for exploration of novel therapies to inhibit angiogenesis. These could include blockade of the VEGFR, a receptor of great importance to the growth and development of endothelial cells, with tyrosine kinase inhibitors, anti–VEGFR antibody, or VEGFR immunization [33–36]. The expression of c-kit by SB-HSA cells may also offer an opportunity to pursue novel tyrosine kinase inhibitors that have shown remarkable efficacy against several human and canine cancers that express c-kit [37,38]. Likewise, the adhesion molecule ($\alpha_v\beta_3$ integrin) we identified on SB-HSA cells presents yet another potential target to study treatments intended to disrupt its function such as the $\alpha_v\beta_3$ integrin–blocking antibody, LM609, or its human chimerized form, Vitaxin, which is being evaluated in human clinical trials [39,40].

We chose to investigate the ability of IL-12 to suppress the growth of SB-HSA tumors. This question was of interest for several reasons. IL-12 reportedly exerts antiangiogenic effects. This activity is mediated by several chemokines (e.g., IP-10, Mig) that are induced in response to interferon-γ elicited by IL-12 [41,42]. In our system, we wanted to evaluate the capacity of IL-12 to inhibit the growth of an endothelial malignancy. We determined that IL-12 significantly inhibited the growth of this tumor in mice. The strain of mice used in these experiments (NOD-SCID), although immunocompromised, possesses NK cells that secrete interferon-γ in response to IL-12 (data not shown). Others have also shown that SCID mice maintain the ability to respond to IL-12 by increasing both serum levels of IFN-γ and IFN-γ transcription in splenocytes and that these responses are mediated by NK cells [43]. We did not determine whether induction of antiangiogenic chemokines by IL-12 suppressed growth of SB-HSA tumors directly. It is possible that IL-12 augmented the cytotoxic capacity of the NK cells, which, in turn, mediated destruction of the xenografted tumor implants [44]. However, an investigation of the therapeutic effect of IL-12 on mouse hemangiosarcomas determined that interferon-γ, and not cytotoxic lymphocytes, was responsible for suppressing the proliferation of malignant murine endothelial cells [45]. Still others have reported an effect of IL-12 on promoting the apoptosis of endothelial cells [46]. Taken together, these various possibilities may account for the promise that IL-12 has shown as a treatment for aggressive endothelial cell malignancies such as Kaposi sarcoma [47]. Similarly, intralesional injection of IL-2 has been used successfully as a treatment for cutaneous hemangiosarcoma in humans [48–50]. Thus, there is active interest in exploring a role for immunostimulatory cytokines in controlling endothelial malignancies. Because of the numerous potential mechanisms through which IL-12 can affect endothelial cell growth, it is particularly interesting for this purpose as well as for the suppression of endothelial cell growth in other cancers. The endothelial cell model we have described offers unique opportunities to pursue further investigations with IL-12, as well as other antiangiogenic approaches in cancer therapy.

Acknowledgement

We thank Cheryl London (Davis, CA) for the canine c-kit and SCF sequences.

References

[1] Jarrell B, Levine E, Williams S, Carabasi RA, Mueller S, and Thornton S (1984). Human adult endothelial cell culture. *J Vasc Surg* **1,** 757–764.
[2] Simonescu N, and Simonescu M (Eds.) (1988). Endothelial Cell Biology in Health and Disease. Plenum, New York.
[3] Thilo-Korner D, Freshmey RI (Eds.) (1983). In the Endothelial Cell—A Pluripotent Control Cell of the Vessel Wall Karger, Basel.
[4] Obeso J, Weber J, and Auerbach R (1990). A hemangioendothelioma-derived cell line: its use as a model for the study of endothelial cell biology. *Lab Invest* **63,** 259–269.
[5] Gumkowski F, Kaminska G, Kaminski M, Morrissey LW, and Auerbach R (1987). Heterogeneity of mouse vascular endothelium. *In vitro* studies of lymphatic, large blood vessel and microvascular endothelial cells. *Blood Vessels* **24,** 11–23.
[6] Jaffe EA (Ed.) (1983). The Biology of Endothelial Cells. Martinus Nijhoff, The Hague.
[7] Kumar S, West DC, and Ager A (1987). Heterogeneity in endothelial cells from large vessels and microvessels. *Differentiation* **36,** 57–70.
[8] Bouis D, Hospers GA, Meijer C, Molema G, and Mulder NH (2001). Endothelium *in vitro*: a review of human vascular endothelial cell lines for blood vessel–related research. *Angiogenesis* **4,** 91–102.
[9] Kemmner W, Schlag P, and Brossmer R (1987). A rapid and simple procedure for dissociation of tumor tissue from the human colon. *J Cancer Res Clin Oncol* **113,** 400–401.
[10] Solovey A, Lin Y, Browne P, Choong S, Wayner E, and Hebbel RP (1997). Circulating activated endothelial cells in sickle cell anemia. *N Engl J Med* **337,** 1584–1590.
[11] Illera MJ, Lorenzo PL, Gui YT, Beyler SA, Apparao KB, and Lessey BA (2003). A role for alpha v beta 3 integrin during implantation in the rabbit model. *Biol Reprod* **68,** 766–771.
[12] Sipkins DA, Cheresh DA, Kazemi MR, Nevin LM, Bednarski MD, and Li KC (1998). Detection of tumor angiogenesis *in vivo* by alphaVbeta3-targeted magnetic resonance imaging. *Nat Med* **4,** 623–626.
[13] Fox RJ, and Frame MD (2002). Arteriolar flow recruitment with vitronectin receptor stimulation linked to remote wall shear stress. *Microvasc Res* **64,** 414–424.
[14] Frame MD, Miano JM, Yang J, and Rivers RJ (2001). Localized adenovirus-mediated gene transfer into vascular smooth muscle in the hamster cheek pouch. *Microcirculation* **8,** 403–413.
[15] Bhattacharya SRP, Sen N, Quadri S, Parthasarathi K, and Bhattacharya J (2001). Dual signaling by the alphavbeta3-integrin activates cytosolic PLA2 in bovine pulmonary artery endothelial cells. *Am J Physiol Lung Cell Mol Physiol* **280,** L1049–1056.
[16] Leven RM, and Tablin F (1992). Extracellular matrix stimulation of guinea pig megakaryocyte proplatelet formation *in vitro* is mediated through the vitronectin receptor. *Exp Hematol* **20,** 1316–1322.
[17] Miyauchi A, Alvarez J, Greenfield EM, Teti A, Grano M, Colucci S, Zambonin-Zallone A, Ross FP, Teitelbaum SL, and Cheresh DA (1991). Recognition of osteopontin and related peptides by an alpha v beta 3 integrin stimulates immediate cell signals in osteoclasts. *J Biol Chem* **266,** 20369–20374.
[18] Cheresh DA (1987). Human endothelial cells synthesize and express an Arg–Gly–Asp–directed adhesion receptor involved in attachment to fibrinogen and von Willebrand factor. *Proc Natl Acad Sci* **84,** 6471–6475.
[19] Ritt MG, Mayor J, Wojcieszyn J, Smith R, Barton CL, and Modiano JF (2000). Sustained nuclear localization of p21/WAF-1 upon growth arrest induced by contact inhibition. *Cancer Lett* **158,** 73–84.
[20] Koenig A, Fosmire S, Bianco S, Wojcieszyn J, and Modiano JF (2002). Expression and significance of p53, Rb, p21/Waf-1, p16/Ink-4a, and PTEN tumor suppressors in canine melanoma. *Vet Pathol* **39,** 458–472.
[21] Breen M, Langford CF, Carter NP, Holmes NG, Dickens HF, Thomas R, Suter N, Ryder EJ, Pope M, and Binns MM (1999). FISH mapping and identification of canine chromosomes. *J Hered* **90,** 27–30.
[22] Muthukkaruppan V, and Auerbach R (1979). Angiogenesis in the mouse cornea. *Science* **205,** 1416–1418.
[23] Kenyon BM, Voest EE, Chen CC, Flynn E, Folkman J, and D'Amato RJ (1996). A model of angiogenesis in the mouse cornea. *Invest Ophthalmol Vis Sci* **37,** 1625–1632.

[24] Akhtar N, Dickerson EB, and Auerbach R (2002). The sponge/Matrigel angiogenesis assay. *Angiogenesis* **5,** 75–80.
[25] Auerbach R, Lewis R, Shinners B, Kubai L, and Akhtar N (2003). Angiogenesis assays: a critical overview. *Clin Chem* **49,** 32–40.
[26] Brown NO, Patnaik AK, and MacEwen EG (1985). Canine hemangiosarcoma: retrospective analysis of 104 cases. *J Am Vet Med Assoc* **186,** 56–58.
[27] Priester WA, and McKay FW (1980). The occurrence of tumors in domestic animals. *Natl Cancer Inst Monogr* **54,** 1–210.
[28] Oksanen A (1978). Haemangiosarcoma in dogs. *J Comp Pathol* **88,** 585–595.
[29] Hammer AS, Couto CG, Filppi J, Getzy D, and Shank K (1991). Efficacy and toxicity of VAC chemotherapy (vincristine, doxorubicin, and cyclophosphamide) in dogs with hemangiosarcoma. *J Vet Intern Med* **5,** 160–166.
[30] Sorenmo KU, Jeglum KA, and Helfand SC (1993). Chemotherapy of canine hemangiosarcoma with doxorubicin and cyclophosphamide. *J Vet Intern Med* **7,** 370–376.
[31] Holden CA, Spittle MF, and Wilson Jones E (1987). Hemangiosarcoma of the face and scalp, prognosis and treatment. *Cancer* **59,** 1046–1057.
[32] Morrison WH, Byers RM, Garden AS, Evans HL, Kian Ang K, and Peters LJ (1995). Cutaneous angiosarcoma of the head and neck. *Cancer* **76,** 319–327.
[33] Bergerrs G, Song S, Meyer-Morse N, Bergsland E, and Hanahan D (2003). Benefits of targeting both pericytes and endothelial cells in the tumor vasculature with kinase inhibitors. *J Clin Invest* **111,** 1287–1295.
[34] Kunkelm P, Ulbricht U, Bohlen P, Brockmann MA, Fillbrandt R, Stavrou M, Westphal M, and Lamzus K (2001). Inhibition of glioma angiogenesis and growth *in vivo* by systemic treatment with a monoclonal antibody against vascular endothelial growth factor receptor-2. *Cancer Res* **61,** 6624–6628.
[35] Zhu Z, Hattori K, Zhang H, Jimenez X, Ludwig DL, Dias S, Kussie P, Koo H, Kim HJ, Lu D, Liu M, Tejada R, Friedrich M, Bohlen P, Witte L, and Rafi S (2003). Inhibition of human leukemia in an animal model with human antibodies directed against vascular endothelial growth factor receptor 2. Correlation between antibody affinity and biological activity. *Leukemia* **17,** 604–611.
[36] Li Y, Wang MN, Li H, King KD, Bassi R, Sun H, Santiago A, Hooper AT, Bohlen P, and Hicklin DJ (2002). Active immunization against the vascular endothelial growth factor receptor flk1 inhibits tumor angiogenesis and metastasis. *J Exp Med* **195,** 1575–1584.
[37] Dematteo RP, Heinrich MC, El-Rifai WM, and Demerti G (2002). Clinical management of gastrointestinal stromal tumors: before and after STI-571. *Hum Pathol* **33,** 466–477.
[38] Liao AT, Chien MB, Shenoy N, Mendel DB, McMahon G, Cherrington JM, and London CA (2002). Inhibition of constitutively active forms of mutant kit by multitargeted indolinone tyrosine kinase inhibitors. *Blood* **100,** 585–593.
[39] Gutheil JC, Campbell TN, Pierce PR, Watkins JD, Huse WD, Bodkin DJ, and Cheresh DA (2000). Targeted antiangiogenic therapy for cancer using vitaxin: a humanized monoclonal antibody to the integrin avb3. *Clin Cancer Res* **6,** 3056–3061.
[40] Patel SR, Jenkins J, Papadopolous N, Burgess MA, Plager C, Gutterman J, and Benjamin RS (2001). Pilot study of vitaxin—an angiogenesis inhibitor in patients with leiomyosarcomas. *Cancer* **92,** 1347–1348.
[41] Angiolillo AL, Sgadari C, and Tosato G (1996). A role for the interferon-inducible protein 10 in inhibition of angiogenesis by interleukin-12. *Ann NY Acad Sci* **795,** 158–167.
[42] Sgadari C, Angiolillo AL, and Tosato G (1996). Inhibition of angiogenesis by interleukin-12 is mediated by the interferon-inducible protein 10. *Blood* **87,** 3877–3882.
[43] Carson WE, Dierksheide JE, Jabbour S, Anghelina M, Bouchard P, Ku G, Yu H, Baumann H, Shah MH, Cooper MA, Durbin J, and Caligiuri MA (2000). Coadministration of interleukin-18 and interleukin-12 induces a fatal inflammatory response in mice: critical role of natural killer cell interferon-γ production and STAT-mediated signal transduction. *Blood* **96,** 1465–1473.
[44] Yao L, Sgadari C, Furuke K, Bloom ET, Teruya-Feldstein J, and Tosato G (1999). Contribution of natural killer cells to inhibition of angiogenesis by interleukin-12. *Blood* **93,** 1612–1621.
[45] Vizler C, Rosato A, Calderazzo F, Quinitieri L, Fruscella P, Wainstok de Calmanovici R, Mantovani A, Vecchi A, Zanovelio P, and Coliavo D (1998). Therapeutic effect of interleukin 12 on mouse haemangiosarcomas is not associated with an increased anti-tumour cytotoxic T-lymphocyte activity. *Br J Cancer* **77,** 656–662.
[46] Duda DG, Sunamura M, Lozonachi L, Kodama T, Egawa S, Matsumoto G, Shimamura H, Shibuya K, Takeda K, and Matsumo S (2000). Direct *in vitro* evidence and *in vivo* analysis of the antiangiogenesis effects of interleukin 12. *Cancer Res* **60,** 1111–1116.
[47] Gascon P, and Schwartz RA (2000). Kaposi's sarcoma. New treatment modalities. *Dermatol Clin* **18,** 169–175.
[48] Masuzawa M, Higashi K, Nishioka K, and Nishiyama S (1988). Successful immunotherapy for malignant hemangioendothelioma using recombinant interleukin-2. *Jpn J Dermatol* **98,** 367–369.
[49] Inadomi T, Fujioka A, and Suzuki H (1992). A case of malignant hemangioendothelioma showing response to interleukin-2 therapy. *Br J Dermatol* **127,** 442–449.
[50] Masuzawa M, Mochida N, Amano T, Fujimura T, Hamada V, Tamauchi H, Sakurai Y, Nishiyama S, and Katsuoka K (2001). Evaluation of recombinant interleukin-2 immunotherapy for human hemangiosarcoma in a SCID mouse model (WB-SCID). *J Dermatol Sci* **27,** 88–94.